

AGC 226067: A possible interacting low-mass system

E. A. K. Adams¹, J. M. Cannon², K. L. Rhode³, W. F. Janesh³, S. Janowiecki³, L. Leisman⁴, R. Giovanelli⁴, M. P. Haynes⁴, T. A. Oosterloo¹, J. J. Salzer³, and T. Zaidi²

¹ ASTRON, Netherlands Institute for Radio Astronomy, Postbus 2, 7900 AA Dwingeloo, The Netherlands e-mail: adams@astron.nl

² Department of Physics and Astronomy, Macalaster College, 1600 Grand Avenue, Saint Paul, MN 55105, USA

³ Department of Astronomy, Indiana University, 727 East Third Street, Bloomington, IN 47405, USA

⁴ Center for Radiophysics and Space Research, Space Sciences Building, Cornell University, Ithaca, NY 14853, USA

June 3, 2021

ABSTRACT

We present Arecibo, GBT, VLA and WIYN/pODI observations of the ALFALFA source AGC 226067. Originally identified as an ultra-compact high velocity cloud and candidate Local Group galaxy, AGC 226067 is spatially and kinematically coincident with the Virgo cluster, and the identification by multiple groups of an optical counterpart with no resolved stars supports the interpretation that this system lies at the Virgo distance ($D = 17$ Mpc). The combined observations reveal that the system consists of multiple components: a central H α source associated with the optical counterpart (AGC 226067), a smaller H α -only component (AGC 229490), a second optical component (AGC 229491), and extended low surface brightness H α . Only $\sim 1/4$ of the single-dish H α emission is associated with AGC 226067; as a result, we find $M_{\text{HI}}/L_g \sim 6 M_{\odot}/L_{\odot}$ which is lower than previous work. At $D = 17$ Mpc, AGC 226067 has an H α mass of $1.5 \times 10^7 M_{\odot}$ and $L_g = 2.4 \times 10^6 L_{\odot}$, AGC 229490 (the H α -only component) has $M_{\text{HI}} = 3.6 \times 10^6 M_{\odot}$, and AGC 229491 (the second optical component) has $L_g = 3.6 \times 10^5 L_{\odot}$. The nature of this system of three sources is uncertain: AGC 226067 and AGC 229490 may be connected by an H α bridge, and AGC 229490 and AGC 229491 are separated by only 0.5'. The current data do not resolve the H α in AGC 229490 and its origin is unclear. We discuss possible scenarios for this system of objects: an interacting system of dwarf galaxies, accretion of material onto AGC 226067, or stripping of material from AGC 226067.

Key words. galaxies: dwarf — galaxies: ISM — radio lines: galaxies

1. Introduction

The ALFALFA H α survey offers a census of neutral hydrogen (H α) in the nearby Universe (Giovanelli et al. 2005). Due to its sensitivity and footprint area, ALFALFA has been able to detect rare but extremely interesting objects, including H α sources that probe the extreme limits of systems that are able to form stars. These sources can be coarsely separated into three types: the candidate gas-rich but (nearly) starless Local Group galaxies, called “ultra-compact high velocity clouds” or “UCHVCs” (Giovanelli et al. 2010; Adams et al. 2013, hereafter A13); the low-mass, gas-rich “SHIELD” dwarf galaxies (Cannon et al. 2011); the clearly extragalactic H α detections with no discernible optical counterpart in extant optical surveys, called “Almost-Dark” sources (Janowiecki et al. 2015; Cannon et al. 2015, Leisman et al., in prep.).

AGC 226067 is an ALFALFA source that highlights the extreme objects contained within these samples. It was included in the UCHVC catalogs of Giovanelli et al. (2010) and A13 (as HVC274.68+74.70-123) due to its low recessional velocity ($cz_{\odot} = -128 \text{ km s}^{-1}$), small angular extent ($5' \times 4'$) and isolation from other high-velocity clouds. However, AGC 226067 is projected onto the Virgo Cluster along with at least 14 galaxies located within 3° and 100 km s^{-1} . Two of these systems have Tully-Fisher distances consistent with the distance to Virgo: NGC 4396 (Gavazzi et al. 1999, $D = 15.8$ Mpc) and IC 3311 (Parnovsky & Parnowski 2010, $D = 21.1$ Mpc). The detection by Bellazzini et al. (2015, hereafter B15) and Sand et al. (2015, hereafter S15) of an optical counterpart to AGC 226067 with-

out resolved stars in ground-based imaging implies $D \gtrsim 3$ Mpc, negating its identification as an UCHVC and making the association with the Virgo Cluster likely. We assume throughout this work that AGC 226067 is located in the Virgo Cluster at $D = 17$ Mpc. If it is located closer, it is a lower mass system.

In this paper we present global single-dish H α spectra, resolved H α imaging with the *Karl G. Jansky* Very Large Array (VLA), and deep optical imaging with WIYN/pODI of AGC 226067. Our observations definitively associate the H α with the optical counterpart as a low mass dwarf irregular, analogous to the SHIELD galaxies. Importantly, these data reveal that AGC 226067 is an extended interacting system with multiple components, both H α and optical.

2. Data

2.1. Single-dish H α data

AGC 226067 was originally detected in the Arecibo Legacy Fast ALFA (ALFALFA) H α line survey and is included in the catalogs of Giovanelli et al. (2007) and Haynes et al. (2011); full details of source extraction are given in those works. Due to the lack of an optical counterpart and the low recessional velocity, this source was also included in the UCHVC catalogs of Giovanelli et al. (2010) and A13. In the work of A13, the sources were independently re-measured to ensure that the extended, diffuse emission common to the UCHVCs was properly included, resulting in a flux density that was 15% higher than given by Haynes et al. (2011).

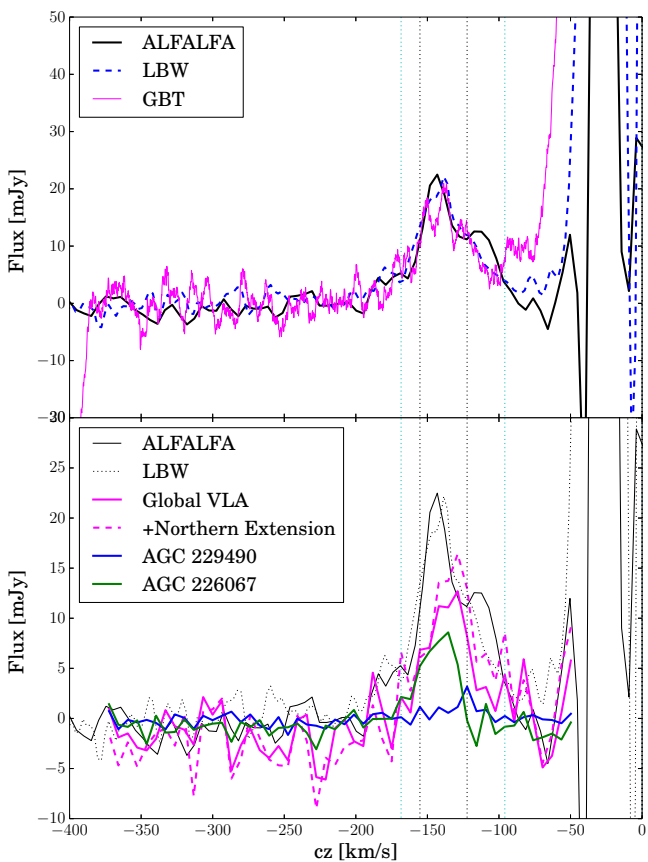


Fig. 1. Top: The single-dish spectra for AGC 226067. Both the ALFALFA and LBW spectrum are Hanning smoothed to a velocity resolution of 10 km s^{-1} , and the GBT spectrum is boxcar smoothed to a resolution of 5 km s^{-1} . Dotted lines indicate the two velocity ranges used for constructing the VLA total H₁ intensity maps. Bottom: The global VLA spectrum, including with the potential northern extension, along with the isolated spectra for AGC 226067 and AGC 229490. The ALFALFA and LBW spectra are included for reference.

AGC 226067 was also observed with both the L-band wide receiver (LBW) at Arecibo Observatory (AO; 22 March 2013, program A2752) and the *Robert C. Byrd* Green Bank Telescope (GBT; 23 October 2012, program GBT/12B-059) as part of programs aimed at confirming UCHVCs. The LBW observation was a 3 minute ON-OFF position switching pair, and the GBT observation was a 15 minute track in frequency-switching mode. Both spectra were calibrated with observatory-provided routines and the baseline-subtracted spectra are shown in the upper panel of Figure 1, along with the ALFALFA spectrum from A13.

Table 1 reports the global H₁ properties from the single-dish spectra. The LBW spectrum matches the ALFALFA spectrum well but lacks the bump in emission in the red-wing of the profile. Consequently, the measured velocity width and flux density are slightly lower but still consistent with the ALFALFA data. The ALFALFA source size is more extended than the AO beam, so the missing emission could be outside the LBW pointing. However, the GBT beam encompasses the full source extent of AGC 226067. While the GBT spectrum is much noisier, it is a good match to the LBW spectrum, indicating that the lack of red-wing emission may be real and the majority of emission is located within the AO beam. Additionally, all the spectra show low amplitude blue-wing emission, indicating that this may be true emission.

Table 1. Global H₁ Properties

Data	S_{HI} Jy km s ⁻¹	cz_{\odot} km s ⁻¹	W_{50} km s ⁻¹
ALFALFA ^a	0.92 ± 0.1	-128 ± 4	54 ± 13
LBW	0.80 ± 0.15	-139 ± 1	48 ± 6
GBT	0.77 ± 0.18	-139 ± 2	48 ± 4
VLA	0.47 ± 0.20	-135 ± 3	34 ± 3
+ Northern extension	0.68 ± 0.20	-133 ± 3	35 ± 6

Notes. ^(a) From A13

2.2. VLA H₁ data

AGC 226067 was observed in July 2014 with the VLA in D-configuration for 3 one-hour blocks, corresponding to 1.7 hours of on-source integration time. The WIDAR correlator was configured to provide a 4 MHz bandwidth subdivided into 1024 channels, corresponding to a native velocity resolution of $0.82 \text{ km s}^{-1} \text{ ch}^{-1}$. Standard calibration of the visibility data was done in AIPS, including bandpass, flux and complex gain calibration. Line-free channels were used to remove the continuum emission.

Imaging was done in CASA using Briggs weighting with a robust value of 0.2; the resulting clean beam was $47.3'' \times 43.8''$. Clean data cubes binned to a velocity resolution of 6.6 km s^{-1} (8 channels) were produced by selecting a clean box that contained all emission from the source and cleaning to 0.5 times the rms (1 mJy bm^{-1}) over the full velocity range of emission (-168.5 to -95.9 km s^{-1}). Total H₁ intensity (moment zero) maps were created for two different velocity ranges: the spectral extent based on the ALFALFA spectrum (-168.5 to -95.9 km s^{-1}) and the spectral extent based on the VLA data (-155.3 to -122.3 km s^{-1}). The spectral extent of the VLA data was determined by spatially smoothing the data cube to a resolution of $100''$ and selecting channels with contiguous emission. Both H₁ maps are shown in Figure 2 and have the same structure: two distinct H₁ components with evidence for low-level emission connecting them. In addition, the full velocity range map also shows a potential northern extension of emission.

In order to include low level emission when finding the flux density, masks were created by smoothing the moment zero maps to $100''$ resolution and clipping at the 3σ level. These masks were then applied to original moment zero maps in order to define regions of emission used for calculating the flux density. The recovered flux density for the full spectral range is $0.47 \text{ Jy km s}^{-1}$. This is 15% higher than that found for the limited velocity range map, indicating that there is low level emission not clearly evident in the edge channels in the VLA data. In addition, for the full velocity range moment zero map, the northern extension is clearly evident in the smoothed map and is tenuously connected to the rest of the emission at the 3σ level. If this is included as part of the source, the total flux density rises to $0.68 \text{ Jy km s}^{-1}$. We discuss this further in Section 3.3.

The source breaks into two distinct H₁ components; we refer to the main, central source as AGC 226067 and assign the smaller, northern source a new identifier in the Arecibo General Catalog (AGC): 229490. We isolate these two sources by clipping the full spectral range H₁ map at the 2.5σ level. The individual spectra of these sources are shown in Figure 1, and the H₁ properties are reported in Table 2. Much of the VLA emission is at low levels surrounding these two sources and is not directly assigned to the individual sources.

We performed a kinematic analysis of the H₁ by fitting Gaussian functions to the spectral data cube using XGAUFT in GIPSY

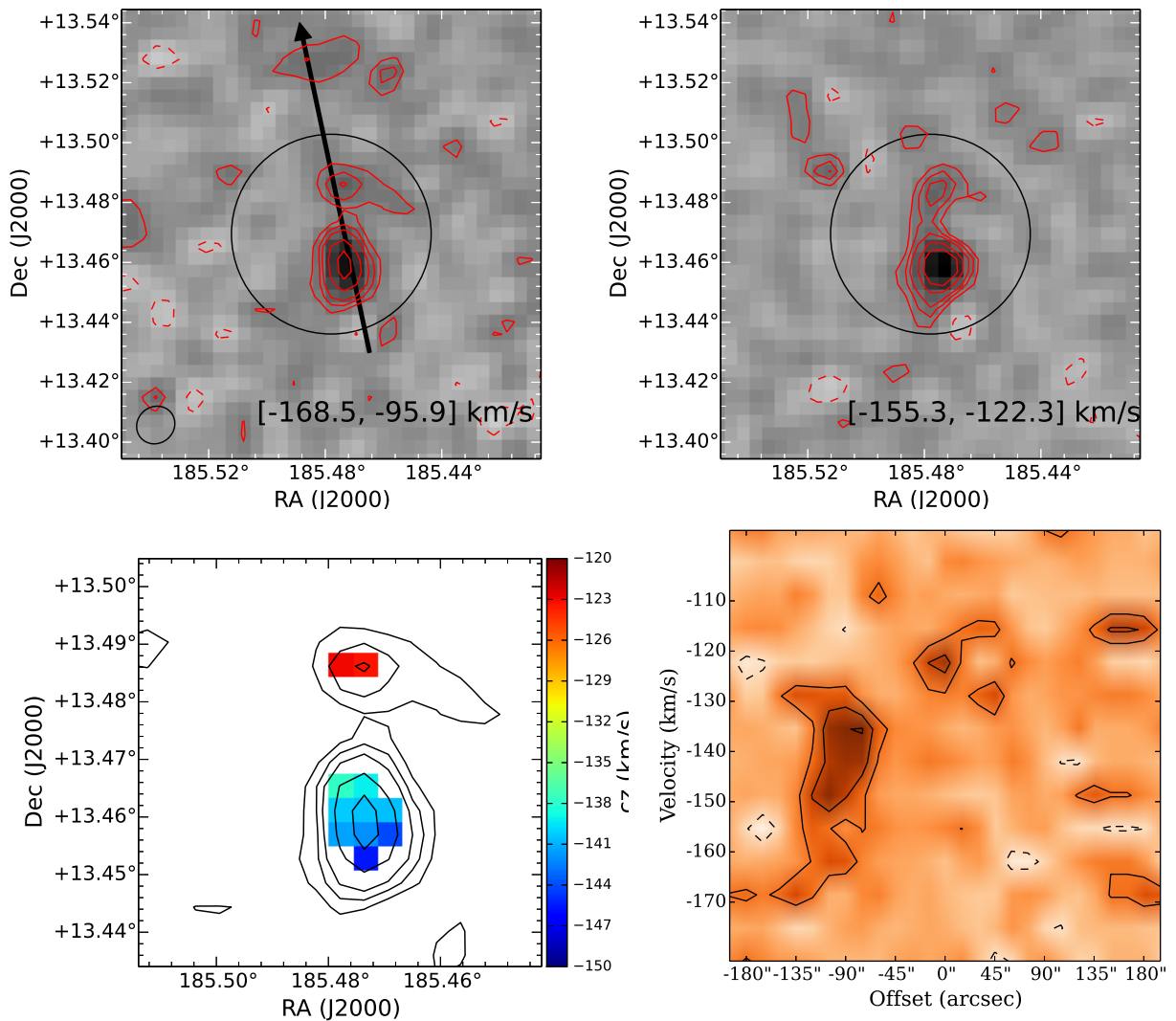


Fig. 2. *Top:* Total intensity H₁ maps for the two channel ranges. Contours show the $(-2, 2, 3, 4, 6, 8) \times \text{rms}$ value for each map (0.018 and 0.015 Jy km s⁻¹). The 4' AO beam is shown as the large circle for reference. The synthesized VLA beam is shown as the small circle in the top-left figure. *Bottom Left:* H₁ intensity contours from the full spectral range H₁ map (upper left) overlaid on the velocity field from Gaussian fitting. *Bottom right:* Position-velocity slice along the arrow shown in the upper left with contours at $(-2, 2, 4, 6) \times \text{rms}$ (1 mJy bm⁻¹).

with the requirement that the peak amplitude be $>5\sigma$ (10 mJy bm⁻¹). The resulting velocity field is shown in Figure 2. AGC 226067 shows evidence for rotation with an amplitude of ~ 15 km s⁻¹. AGC 229490 is offset by 19 km s⁻¹ in central velocity and has narrow fitted velocity dispersions, consistent with the velocity width found in the extracted spectrum but unusual for extragalactic systems. A position-velocity slice bisecting AGC 226067, AGC 229490, and part of the potential northern extension shows that the H₁ components may be continuous in position-velocity space.

We use these data to place limits on the dynamical masses. The velocity dispersion is an important contribution for these systems and we adopt the expression of Hoffman et al. (1996):

$$M_{\text{dyn}} = 2.325 \times 10^5 \left(\frac{V_{\text{rot}}^2 + 3\sigma^2}{\text{km}^2 \text{s}^{-2}} \right) \left(\frac{r}{\text{kpc}} \right) M_{\odot}. \quad (1)$$

For AGC 226067, we adopt a rotational velocity of 15 km s⁻¹, a velocity dispersion of 9 km s⁻¹ based on the Gaussian fitting and W_{50} of the extracted spectrum, and a radius of 4.1 kpc (50'' at 17 Mpc), to find a dynamical mass of $4.5 \times 10^8 M_{\odot}$. For AGC 229490, we assume no rotation and adopt a velocity dispersion

of 4 km s⁻¹ and a radius of 1.6 kpc (20'' at 17 Mpc, slightly smaller than the beam size), giving a dynamical mass estimate of $1.8 \times 10^7 M_{\odot}$. If the velocity width or H₁ size of AGC 229490 is larger than revealed by the low S/N data here, its dynamical mass will also be larger. Conversely, if AGC 229490 is significantly smaller than the beam of these observations, the dynamical mass will decrease.

2.3. WIYN/pODI data

AGC 226067 was observed on 14 March 2013 with the partially populated One Degree Imager (pODI; $\sim 24' \times 24'$ field of view) on the WIYN 3.5m telescope¹. Nine 300-second exposures were obtained in a dither pattern in the SDSS *g* and *i* filters. The data were reduced in the same manner as described in Janowiecki et al. (2015): they were run through the QuickReduce data reduction pipeline (Kotulla 2014) using the ODI Pipeline, Portal,

¹ The WIYN Observatory is a joint facility of the University of Wisconsin-Madison, Indiana University, the University of Missouri, and the National Optical Astronomy Observatory.

Table 2. Source Properties

Property	AGC 226067	AGC 229490	AGC 229491
R.A. (J2000)	12:21:53.6 ^a	12:21:53.8 ^a	12:21:55.9 ^b
Decl. (J2000)	+13:27:32 ^a	+13:29:08 ^a	+13:29:04 ^b
S_{HI} (Jy km s ⁻¹)	0.22 ± 0.06	0.053 ± 0.04	< 0.08
cz_{\odot} (km s ⁻¹)	-142	-123	...
W_{50} (km s ⁻¹)	25 ± 3	10 ± 2	...
σ_{gas} (km s ⁻¹)	9 ± 3	4 ± 2	...
$a \times b$ (H I)	105'' × 75''	45'' × 45'' ^c	...
N_{HI} (atoms cm ⁻²)	8.6×10^{19}	4.0×10^{19}	< 2.8×10^{19}
g_0^d (mag)	20.30 ± 0.03	$\mu_g > 27.6$	22.38 ± 0.03
$(g - i)_0^d$ (mag)	0.58 ± 0.04	...	-0.29 ± 0.08
M_{HI}/L_g^d (M_{\odot}/L_{\odot})	~6	> 40 ^e	< 14
Distance-Dependent Parameters ($D = 17$ Mpc)			
r_{HI} (kpc)	3.7	< 1.6	...
M_{HI} ($10^5 M_{\odot}$)	150	36	< 50 ^f
M_{dyn} ($10^6 M_{\odot}$)	450	18	...
M_{HI}/M_{dyn}	0.03	0.2	...
M_g^d (mag)	-10.85	> -7.2 ^e	-8.77
L_g^d ($10^5 L_{\odot}$)	24	< 0.85 ^e	3.6

Notes. ^(a) H I centroid ^(b) Optical center ^(c) Unresolved by VLA beam ^(d) Corrected for Galactic extinction from Schlafly & Finkbeiner (2011) ^(e) Based on a 3'' aperture and $\mu_g > 27.6$ mag arcsec⁻² ^(f) For an unresolved source with velocity width of 26.4 km s⁻¹

and Archive² interface, reprojected onto a common pixel scale, scaled to a common flux level, and stacked. Photometric calibration was done using SDSS stars in the images; errors on the zero points were <0.02 mag. Figure 3 shows the *g* band image centered on the region of interest.

Figure 4 shows a color image with H I column density contours. The optical counterpart found by B15 (named SECCO 1) and S15 (named ALFALFA-Dw1) is visible and clearly associated with the main H I component, and hence we continue to refer to this source by the original catalog designation, AGC 226067. After carefully masking foreground stars and background galaxies, we measure $g_0 = 20.30 \pm 0.03$ and $(g - i)_0 = 0.58 \pm 0.04$ for an aperture of radius 15'', empirically determined to contain all the emission.

We independently identify the second optical counterpart noted by S15. This source is located near the second H I component (AGC 229490) but offset to the East by ~30'', so we assign it a unique identification number: AGC 229491. For an aperture of radius 3'' encompassing the blue knot of emission that is AGC 229491, we find $g_0 = 22.38 \pm 0.03$ and $(g - i)_0 = -0.29 \pm 0.08$.

There is no optical source apparent at the location of the second H I peak (AGC 229490); by measuring the variation in the background levels at the location of AGC 229490, we place 3- σ surface brightness limits of $\mu_g > 27.6$ and $\mu_i > 26.4$ mag arcsec⁻². If we assume the same optical size as for AGC 229491 (radius of 3''), this corresponds to $g > 24.0$.

3. The Sources

3.1. AGC 226067: A SHIELD-like dwarf galaxy

The VLA data allow an unambiguous identification of the H I in AGC 226067 with the optical counterpart previously identified by B15 and S15. The VLA observations reveal that only part

² The ODI Pipeline, Portal, and Archive system is a joint development project of the WIYN Consortium, Inc., in partnership with Indiana University's Pervasive Technology Institute (PTI) and with the National Optical Astronomy Observatory Science Data Management Program.

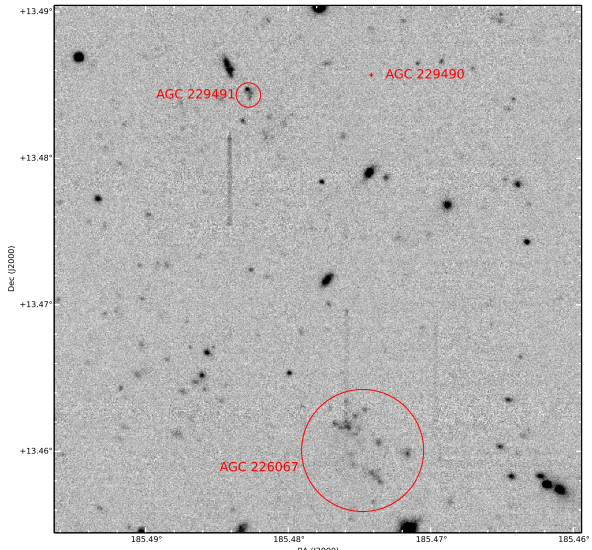


Fig. 3. The WIYN/pODI *g* band image centered on the three sources of interest. The circles indicate the apertures used for photometry for AGC 226067 and AGC 229491, and the red cross marks centroid of the H I-only component, AGC 229490.

of the H I emission detected by ALFALFA is associated directly with AGC 226067, and the H I mass is thus reduced from values based on the single-dish H I emission by a factor of ~4 to $1.5 \times 10^7 M_{\odot}$. Correspondingly, this lowers the M_{HI}/L_V of B15 to ~5 and the M_{HI}/M_* of S15 to ~8. From our pODI data we find $M_{HI}/L_g \sim 6$.

In many ways, AGC 226067 is typical of low mass gas-rich dwarfs, as exemplified by the SHIELD sample of galaxies. The apparent optical extent in our images is 25'', or ~2.1 kpc, typical of low mass dwarf galaxies. The total H I mass of $1.5 \times 10^7 M_{\odot}$ and rotational amplitude of ~15 km s⁻¹ are consistent with the properties of the SHIELD galaxies (Cannon et al. 2011; McQuinn et al. 2014). However, AGC 226067 is distinguished by its lower surface brightness, its companions, and extended H I disk.

3.2. AGC 229490 and AGC 229491

The VLA and deep optical data reveal two additional sources: an H I-only source (AGC 229490) and an optical-only source (AGC 229491). Both are separated from AGC 226067 by ~1.6' (8 kpc). AGC 229491 was noted by S15, but they were not able to definitively associate it with the AGC 226067 system. The extended H I nature of this system and the close proximity to AGC 229490 (0.5', or 2.5 kpc), strongly argue for its physical association with the AGC 226067 system. Treating the AGC 229490 and AGC 229491 as independent sources, we place an upper limit on the H I mass of AGC 229491 of $5.4 \times 10^6 M_{\odot}$ by assuming it is unresolved and has a velocity extent of 26.4 km s⁻¹ (4 channels)³, and an upper limit to the luminosity of AGC 229490 of $L_g < 0.85 \times 10^5 L_{\odot}$, assuming the same $r = 3''$ aperture as for AGC 229491.

Given the close proximity of these two sources, it is plausible that they are part of the same system. AGC 229490 could be gas

³ This upper limit is higher than the measured H I mass of AGC 229490 as the velocity width of AGC 229490 is smaller than assumed here.

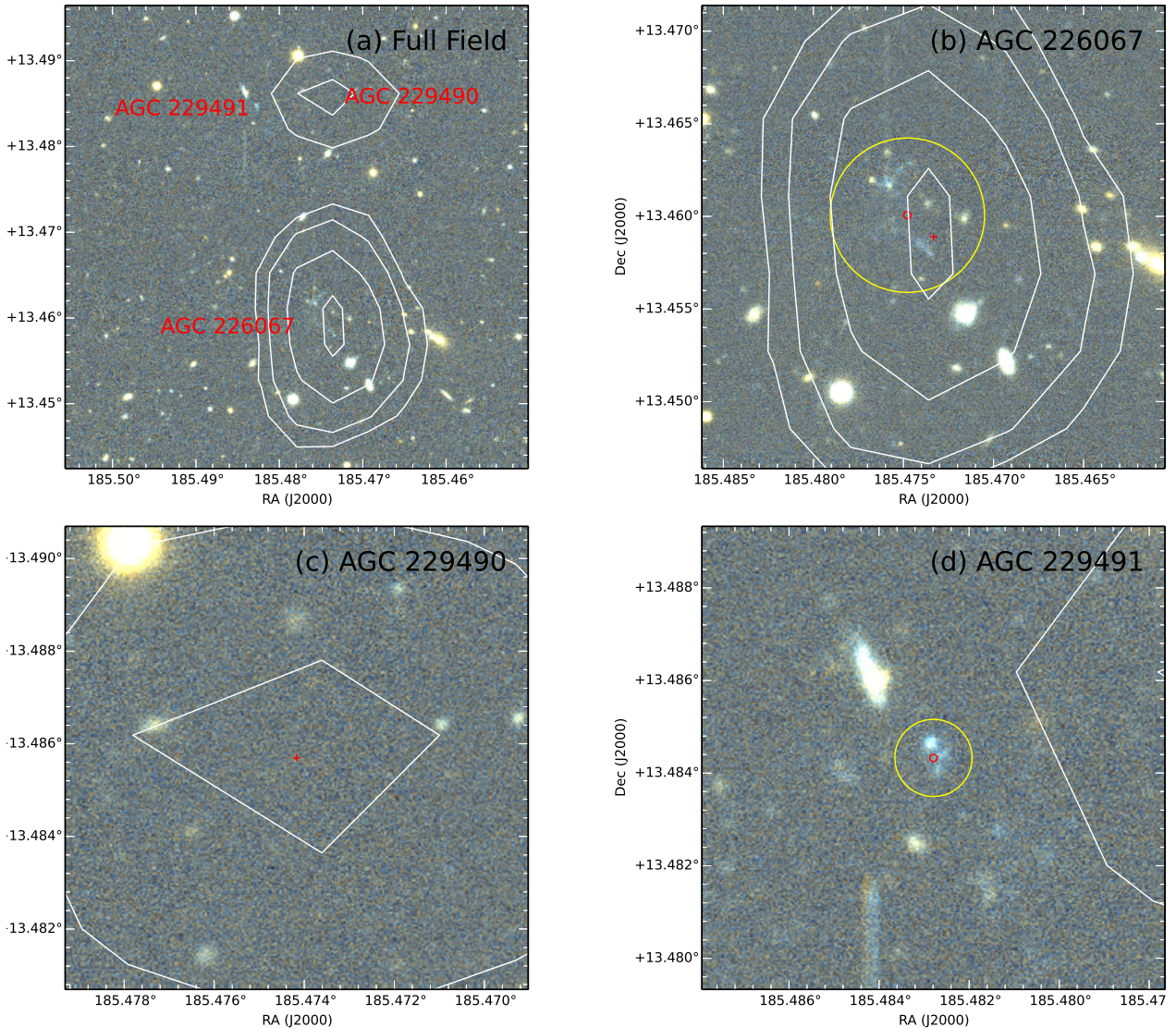


Fig. 4. H₁ column density contours at $(2.5, 3.5, 5.5, 8) \times 10^{19}$ atoms cm⁻² overlaid on a WIYN/pODI color image. The upper left panel shows the full system, the upper right AGC 226067, the lower left AGC 229490 (H₁-only) and the lower right AGC 229491 (optical only). H₁ centroids are marked with crosses and optical centroids with circles. The yellow circles indicate the apertures used for photometry.

that has been removed from AGC 229491, either through internal or external processes. Alternatively, AGC 229490 and AGC 229491 could be bright peaks of the H₁ and stellar distribution within the same dark matter halo. Indeed AGC 229490 shows evidence for an extended H₁ tail at a low (2σ) level (see Figure 2). If we consider the two sources associated, we find a global M_{HI}/L_g value of ~ 10 .

The $M_{\text{HI}}/M_{\text{dyn}}$ value for AGC 229490, while uncertain due to the low resolution and S/N of the VLA data, is 0.2, an unusually high value for dwarf galaxies. This raises the question: is this gas in a dark matter halo or free-floating H₁? Higher resolution and deeper H₁ data, along with deeper optical data, are needed to fully understand AGC 229490 and AGC 229491 and their relation to AGC 226067.

3.3. Potential Extended Emission

The H₁ emission seen in the VLA data around AGC 226067 and AGC 229490 only accounts for $\sim 50\text{--}60\%$ of the H₁ flux seen in the single-dish observations (Table 1), although the VLA data

are shallower than the single-dish observations and the reported flux densities are formally consistent within the errors. There is potentially a significant amount of emission (0.21 Jy km s⁻¹) contained in a northern extension. The VLA spectrum including this extension is shown in Figure 1, and it does a better job of matching the red edge of emission in the single-dish spectra. However, this emission is low S/N and separated from the main body of emission, so it is not clear whether this is real emission.

Given the extended, interacting nature of this system it is quite plausible that there is low surface brightness emission not recovered by the VLA observations. To test this, we adopt the largest discrepancy of 0.45 Jy km s⁻¹ (between the ALFALFA flux density and the VLA flux density⁴). Averaged over an AO beam ($4'$), this corresponds to a column density of 8.6×10^{18} atoms cm⁻², below the sensitivity of these VLA images (rms = 9.5×10^{18} atoms cm⁻²).

⁴ Including the northern extension or adopting the LBW/GBT flux density value reduces the discrepancy between the VLA and single-dish flux density values.

4. Summary and Discussion

Our combined data reveal that the ALFALFA H_I source AGC 226067 is in fact an intriguing system of at least three distinct components plus diffuse H_I emission. Given its kinematic and spatial association with the Virgo Cluster, its most likely distance is $D = 17$ Mpc. The central source, AGC 226067, is a low mass dwarf irregular with extremely low surface brightness, an extended H_I disk, $M_{\text{HI}} = 1.5 \times 10^7 M_{\odot}$, $M_{\text{HI}}/L_g \sim 6$, and $M_{\text{HI}}/M_{\text{dyn}} = 0.03$. The H_I-only source, AGC 229490, is possibly connected to AGC 226067 via an H_I bridge and has $M_{\text{HI}} = 3.6 \times 10^6 M_{\odot}$ and $M_{\text{HI}}/M_{\text{dyn}} \sim 0.2$. The second optical source, AGC 229491, is extremely blue, consistent with a young stellar population, has $L_g = 3.6 \times 10^5 L_{\odot}$, and is offset from AGC 229490 by only 0.5'. The H_I data give a strong indication that this system is undergoing some form of interaction. The evidence supporting an interaction includes the putative H_I bridge, a possible H_I tail as part of AGC 229490, and the potential extended emission to the North. However, the precise nature of that interaction is uncertain. Deeper and higher resolution data, both H_I and optical, are needed to fully address the origin of this system. Here we take a preliminary look at three possibilities:

- Multiple dwarf galaxy system: AGC 226067, AGC 229490 and AGC 229491 are two or three interacting dwarf galaxies. One possibility is that the AGC 229490/91 system is a single dwarf galaxy that passed through AGC 226067, resulting in the offset of the gas and stars through ram pressure. This is consistent with the potential H_I tail of AGC 229490. It is difficult to explain the regular H_I appearance of AGC 226067 in this scenario, but deeper H_I observations may reveal an irregular H_I morphology.
- Accretion onto AGC 226067: AGC 229490 is not gas in a dark matter halo but rather is H_I being accreted onto AGC 226067. In this case, AGC 226067 may be undergoing triggered star formation and only recently have developed an optical counterpart, previously being “too shy to shine”. However, this scenario does not explain AGC 229491.
- Disruption of AGC 226067: AGC 229490 and AGC 229491 were originally part of AGC 226067, but have been stripped from the central galaxy, either through tidal effects or ram pressure. It is not clear what interaction could have led to the projected orientations of the three components.

It is worth noting that several other systems with extreme M_{HI}/L values lie toward the Virgo Cluster, though they are projected further from the cluster center than AGC 226067. This includes HI1225+01, a star-forming dwarf and a dark H_I cloud (Chengalur et al. 1995; Salzer et al. 1991), AGC 226178, a dwarf galaxy with a faint optical counterpart offset from a second H_I-poor dwarf galaxy (Cannon et al. 2015), and HI1232+20, a system of three H_I components of which only one has a detected low surface brightness counterpart (Janowiecki et al. 2015).

Acknowledgements. We thank M. Johnson for support of the GBT observations, D. Harbeck for support of the WIYN/pODI observations, and the anonymous referee for valuable input. The National Radio Astronomy Observatory is a facility of the National Science Foundation operated under cooperative agreement by Associated Universities, Inc. Based on observations at Kitt Peak National Observatory, National Optical Astronomy Observatory (NOAO Prop. ID:2013A-0253; PI:Adams), which is operated by the Association of Universities for Research in Astronomy (AURA) under a cooperative agreement with the National Science Foundation. The ALFALFA work at Cornell is supported by NSF grants AST-0607007 and AST-1107390 to R.G. and M.P.H. and by grants from the Brinson Foundation. K.L.R. and W.F.J. acknowledge support from NSF CAREER award AST-0847109. J.M.C. is supported by NSF grant AST-1211683. This research made use of APLpy, an open-source plotting package for Python hosted at <http://aplpy.github.com>; Astropy, a community-developed core Python package

for Astronomy (Astropy Collaboration, 2013); and NASA’s Astrophysics Data System.

References

- Adams, E. A. K., Giovanelli, R., & Haynes, M. P. 2013, ApJ, 768, 77
 Bellazzini, M., Magrini, L., Mucciarelli, A., et al. 2015, ApJ, 800, L15
 Cannon, J. M., Giovanelli, R., Haynes, M. P., et al. 2011, ApJ, 739, L22
 Cannon, J. M., Martinkus, C. P., Leisman, L., et al. 2015, AJ, 149, 72
 Chengalur, J. N., Giovanelli, R., & Haynes, M. P. 1995, AJ, 109, 2415
 Gavazzi, G., Boselli, A., Scodéglio, M., Pierini, D., & Belsole, E. 1999, MNRAS, 304, 595
 Giovanelli, R., Haynes, M. P., Kent, B. R., & Adams, E. A. K. 2010, ApJ, 708, L22
 Giovanelli, R., Haynes, M. P., Kent, B. R., et al. 2005, AJ, 130, 2598
 Giovanelli, R., Haynes, M. P., Kent, B. R., et al. 2007, AJ, 133, 2569
 Haynes, M. P., Giovanelli, R., Martin, A. M., et al. 2011, AJ, 142, 170
 Hoffman, G. L., Salpeter, E. E., Farhat, B., et al. 1996, ApJS, 105, 269
 Janowiecki, S., Leisman, L., Józsa, G., et al. 2015, ApJ, 801, 96
 Kotulla, R. 2014, in ASP Conf. Ser., Vol. 485, Astronomical Data Analysis Software and Systems XXIII, ed. N. Manset & P. Forshay, 375
 McQuinn, K. B. W., Cannon, J. M., Dolphin, A. E., et al. 2014, ApJ, 785, 3
 Parnovsky, S. L. & Parnowski, A. S. 2010, Ap&SS, 325, 163
 Salzer, J. J., di Serego Alighieri, S., Matteucci, F., Giovanelli, R., & Haynes, M. P. 1991, AJ, 101, 1258
 Sand, D. J., Crnojević, D., Bennet, P., et al. 2015, ApJ, 806, 95
 Schlafly, E. F. & Finkbeiner, D. P. 2011, ApJ, 737, 103